



HAL
open science

Large exchange-dominated domain wall velocities in antiferromagnetically coupled nanowires

Majd Kuteifan, M V Lubarda, S. Fu, R Chang, M A Escobar, S. Mangin, E. Fullerton, V. Lomakin

► **To cite this version:**

Majd Kuteifan, M V Lubarda, S. Fu, R Chang, M A Escobar, et al.. Large exchange-dominated domain wall velocities in antiferromagnetically coupled nanowires. *AIP Advances*, 2016, 6, 10.1063/1.4945789 . hal-02070472

HAL Id: hal-02070472

<https://hal.univ-lorraine.fr/hal-02070472v1>

Submitted on 18 Mar 2019




HAL is a multi-disciplinary open access archive for the deposit and dissemination of scientific research documents, whether they are published or not. The documents may come from teaching and research institutions in France or abroad, or from public or private research centers.

L'archive ouverte pluridisciplinaire **HAL**, est destinée au dépôt et à la diffusion de documents scientifiques de niveau recherche, publiés ou non, émanant des établissements d'enseignement et de recherche français ou étrangers, des laboratoires publics ou privés.

Large exchange-dominated domain wall velocities in antiferromagnetically coupled nanowires

Cite as: AIP Advances **6**, 045103 (2016); <https://doi.org/10.1063/1.4945789>

Submitted: 06 January 2016 . Accepted: 28 March 2016 . Published Online: 06 April 2016

Majd Kuteifan , M. V. Lubarda, S. Fu , R. Chang, M. A. Escobar , S. Mangin, E. E. Fullerton, and V. Lomakin



View Online



Export Citation



CrossMark

ARTICLES YOU MAY BE INTERESTED IN

[The design and verification of MuMax3](#)

AIP Advances **4**, 107133 (2014); <https://doi.org/10.1063/1.4899186>

[Disruptive effect of Dzyaloshinskii-Moriya interaction on the magnetic memory cell performance](#)

Applied Physics Letters **108**, 112403 (2016); <https://doi.org/10.1063/1.4944419>

[Dynamics of antiferromagnetic skyrmion driven by the spin Hall effect](#)

Applied Physics Letters **109**, 182404 (2016); <https://doi.org/10.1063/1.4967006>



Don't let your writing keep you from getting published!

AIP | Author Services

Learn more today!



Large exchange-dominated domain wall velocities in antiferromagnetically coupled nanowires

Majd Kuteifan,^{1,a} M. V. Lubarda,² S. Fu,¹ R. Chang,¹ M. A. Escobar,¹ S. Mangin,³ E. E. Fullerton,¹ and V. Lomakin¹

¹Center for Magnetic Recording Research, University of California San Diego, La Jolla, California 92093-0401, USA

²Faculty of Polytechnics, University of Donja Gorica, 81000 Podgorica, Montenegro

³Institut Jean Lamour, UMR CNRS 7198, Université de Lorraine, BP 70239, F-54506 Vandoeuvre-les-Nancy, France

(Received 6 January 2016; accepted 28 March 2016; published online 6 April 2016)

Magnetic nanowires supporting field- and current-driven domain wall motion are envisioned for methods of information storage and processing. A major obstacle for their practical use is the domain-wall velocity, which is traditionally limited for low fields and currents due to the Walker breakdown occurring when the driving component reaches a critical threshold value. We show through numerical and analytical modeling that the Walker breakdown limit can be extended or completely eliminated in antiferromagnetically coupled magnetic nanowires. These coupled nanowires allow for large domain-wall velocities driven by field and/or current as compared to conventional nanowires. © 2016 Author(s). All article content, except where otherwise noted, is licensed under a Creative Commons Attribution (CC BY) license (<http://creativecommons.org/licenses/by/4.0/>). [<http://dx.doi.org/10.1063/1.4945789>]

Manipulating magnetic domain walls (DWs) to store and transfer information is envisioned to enable high-density, low-power, non-volatile, and non-mechanical memory, recording and processing systems. Related concepts have been explored in the past, e.g. bubble memory,¹ and are promising for future systems, e.g. racetrack memory² where DWs can be moved by applied magnetic fields³ and/or by currents⁴ via the spin transfer torque (STT) effects.^{5,6} STT arises from the transfer of angular momentum from spin-polarized electrons to the DW magnetic moments and provides particularly attractive opportunities for DW manipulation.⁷ However, there are several obstacles to be overcome to enable these technologies. One obstacle is the Walker breakdown limit,^{8,9} which imposes a maximum velocity on the DW motion at low field or current in magnetic systems posing a major problem in terms of the information transfer and storage speed. The Walker breakdown limit originates from the demagnetization field that imparts to the magnetization a torque, which takes the opposite direction once the applied field and/or current exceed a certain critical value. Below these critical field or current values the DW velocity increases with increasing field or current, whereas above this critical value the DW motion exhibits back and forth oscillations. If the Walker breakdown effect could be eliminated then the increased DW speed would allow a major improvement in terms of data rates. Approaches have been presented for reducing or eliminating the Walker breakdown, such as those based on complex topologies or alternative physical effects,¹⁰⁻¹³ or the use of transverse magnetic fields.¹⁴ However, these approaches may be hard to implement in practical systems.

In this Letter we present numerical simulations and an analytical model of antiferromagnetically coupled nanowires (AFC NWs) subject to applied fields and currents. We find that this structure extends or completely eliminates the Walker breakdown limit for DW motion induced by fields or STT currents. For field-driven DW motion the maximum DW velocities and corresponding applied fields can be much higher than those of single-layer NWs. For STT induced DW motion the

^aemail: makuteif@eng.ucsd.edu

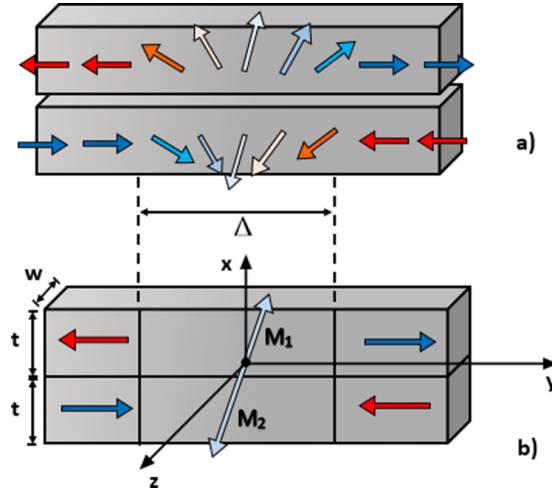


FIG. 1. Schematic of a DW in an AFC NW. (a) The DW represented by a continuous variation of the magnetization states; (b) Representation in the analytical model in which the DW in each layer is represented by a single macrospin with its width w , thickness t , and length Δ .

Walker breakdown can not only be reduced but also eliminated. Importantly, this structure can be readily realized experimentally and enhanced DW velocities have been reported for AFC films with perpendicular anisotropy.¹⁵

The proposed structure is made of two AFC magnetic layers as shown in Fig. 1. The specific model used is made of two soft magnetic NWs antiferromagnetically coupled through their common interface. The saturation magnetization of the first (top) and second (bottom) NWs are M_{s1} and M_{s2} , respectively. The antiferromagnetic coupling between the NWs is sufficiently strong such that a single DW across both NWs is present (Fig. 1). The wire width is chosen relatively small, compatible with the wire sizes envisioned in memory applications. In this case the DW structure is a transverse wall in each layer, with opposite directions. For thicker and wider wires vortex DW should be generated. While similar effects are expected for vortex DWs, the detailed study of this regime is outside the scope of this work. Furthermore, the physical phenomena described for transverse DWs should also be applicable to films with perpendicular magnetic anisotropy.

The dynamics of a DW in a NW under the influence of field and/or current are governed by the Landau-Lifshitz-Gilbert equation extended to include the STT effect:^{7,9}

$$\frac{\partial \mathbf{M}}{\partial t} = \gamma \mathbf{H}_{\text{eff}} \times \mathbf{M} + \frac{\alpha}{M_s} \mathbf{M} \times \frac{\partial \mathbf{M}}{\partial t} - u \frac{\partial \mathbf{M}}{\partial y} + \frac{\beta u}{M_s} \mathbf{M} \times \frac{\partial \mathbf{M}}{\partial y}. \quad (1)$$

In the above equation, \mathbf{M} is the magnetization, γ is the gyromagnetic ratio, \mathbf{H}_{eff} is the effective field, α is the damping parameter, M_s is the saturation magnetization, β is the non-adiabatic spin-transfer parameter, and the parameter u depends on the current density J and is defined as $u = gJ\mu_B P / (2eM_s)$, where g is the Landé factor, μ_B is the Bohr magneton, e is the electron charge, and P is the polarization factor of the current.

The DW dynamics in a single-layer NW governed by Eq. (1) can fall into different regimes depending on the relative values of the parameters. In the absence of current, if the magnitude of the external magnetic field is below the Walker threshold, the wall moves at a constant velocity that increases linearly with field. If the applied field is stronger than this threshold field, there is precession, intervals of backward motion and overall slowdown of the DW propagation. When only current is applied, the dynamics depend on the relative values of the damping parameter α and the non-adiabatic spin-transfer parameter β . If $\beta = \alpha$, the DW motion is steady for any DC applied current. If $\beta > \alpha$, the DW motion is steady for currents smaller than a certain limit, but slows down for stronger currents due to the onset of precession and backward motion. If $\beta < \alpha$, there is a range of low currents for which the spins of the DW tilt out of plane, after which the DW is stationary, i.e.,

no motion. For yet stronger currents, the DW propagates during which its magnetization undergoes precession. All these limits correspond to the Walker threshold that depends on α , the saturation magnetization M_s , and the geometry of the NW.

In an AFC NW system the symmetry of the problem is altered through interlayer exchange fields, which allow compensation of torque terms that lead to the DW instability. The AFC NW geometry significantly reduces the Walker breakdown effects and even eliminates Walker breakdown when current is used to move the DWs via the STT effect. This results in a dramatic increase of the DW velocities in a simple geometry that is practically feasible using different materials such as in-plane anisotropy CoFeB/Ru/CoFeB or Fe/Cr/Fe structures or out-of-plane [Co/Ni]/Ru/[Co/Ni] structures.

The presented simulation results were obtained by solving the LLG equation using both FastMag^{16,17} and OOMMF¹⁸ simulators, which gave nearly identical results. These simulators respectively use finite element method (FEM) and finite differences method and provide a variety of tools that can be used to study DW motion. For each simulation the transverse DW was located inside the NW and its position was monitored. The DW speed in the numerical simulations was obtained by calculating the time for the DW to propagate over a fixed distance (chosen as 10 micron). We studied the evolution of the DW velocity as a function of the applied field in single-layer and AFC NWs for different values of saturation magnetization, damping and exchange fields. For the AFC NW case, each NW had a 4-nm thickness and a 20-nm width. The single-layer NW had a 4-nm thickness and 20-nm width. The mesh was tetrahedral with nearly regular tetrahedrons of side length of 2 nm. The ferromagnetic exchange constant was chosen to be 1.3×10^{-6} erg/cm. In these cases, the values for the damping, non-adiabatic STT parameter and thicknesses of both wires are identical to facilitate comparisons with single wire simulations. However the results can be easily extended to systems where the two layer have different parameters and the conclusions are similar. As a first approximation, increasing the thickness of a layer is roughly equivalent to increasing M_s . This method can be used to create asymmetrical AFC wires using the same material for each wire like the previously described CoFeB/Ru/CoFeB structure.

Figures 2(a) and 2(b) show the DW velocity versus the applied field for single-layer and AFC NW, respectively. The results are given for different damping constants and saturation magnetization values. The magnetocrystalline anisotropy was kept to zero in both models, hence the anisotropy was entirely due to magnetostatics (shape anisotropy). However, this approach is also applicable to perpendicular anisotropy systems. For a single-layer NW, changing the saturation magnetization and damping only affects the DW mobility and the Walker breakdown critical field, but not the maximum achievable DW velocity in the system, as seen from Fig. 2(a). This limitation clearly does not hold for AFC NW (Fig. 2(b)), where the mobility, Walker breakdown critical

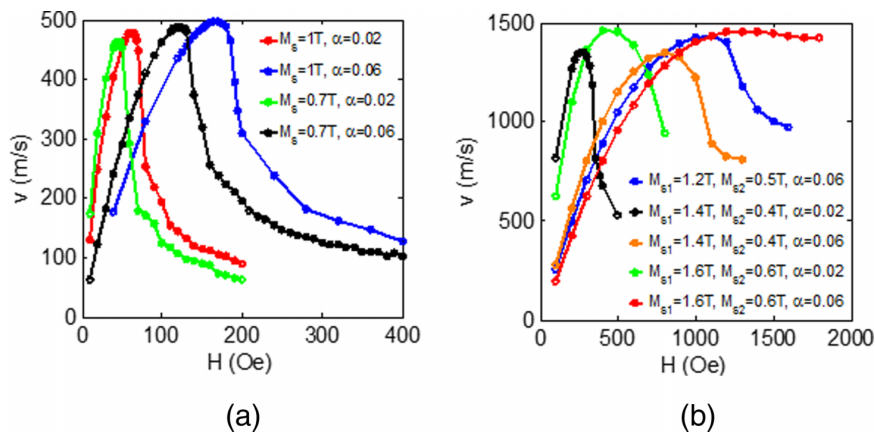


FIG. 2. Average domain velocities (v) driven for applied magnetic field (H) obtained via FEM micromagnetic simulations. (a) single-layer NW with different values of the damping and saturation magnetization; (b) AFC NW with different values of the damping and saturation magnetization with exchange energy density of 10^{-3} J/m².

field, and peak velocity can be modulated through the saturation magnetization and damping of the constituent layers (Fig. 2(b)). Indeed, even when the total saturation magnetization of the composite system $|M_{s1} - M_{s2}|$ is identical to the saturation magnetization of the single-layer NW, the DW motion characteristics are different (Figs. 2(a), 2(b)). The interaction between the two antiferromagnetically coupled layers and the symmetry of the system under the applied field must be taken into account to explain this phenomenon.

Several observations from Fig. 2(b) can be made. First, the closer the saturation magnetizations M_{s1} and M_{s2} are to each other the greater the peak velocity. However, in the pre-Walker breakdown regime, the smaller the net magnetization the slower the DW motion for a given magnetic field. The mobility, defined as the rate of change of DW velocity with the applied field dv/dH , is, therefore, proportional to the net magnetization of the AFC NW. If the saturation magnetization is equal in both layers, there is no motion under an applied field.

The operation of the AFC NW can be understood by considering the compensation of torques in the AF-coupled system, which is mediated through antiferromagnetic interlayer exchange. Indeed, in the strong coupling limit, the directions of the precessional Zeeman torques in each layer are opposite, resulting in a weaker total precessional Zeeman torque $\Gamma_H^{\text{AFC}} \propto M_{s1} - M_{s2}$ acting on the rigid AFC DW. This torque is responsible for the out of plane tilting of the spins, which eventually triggers the Walker breakdown for strong enough applied fields. On the other hand, the direction of the precessional demagnetization and damping torques in each layer complement each other, $\Gamma_d^{\text{AFC}} \propto M_{s1}^2 + M_{s2}^2$ and $\Gamma_\alpha^{\text{AFC}} \propto M_{s1} + M_{s2}$, resulting in a strong torque preventing the Walker breakdown. As a consequence, the Walker breakdown occurs for much greater fields and far greater DW velocities. We note that these modified torque expressions come from the strong coupling assumption, and reflect that the interlayer exchange interaction mediates the dynamical response. A disadvantage to field driven operation, however, is that increases in peak velocities are accompanied with a reduced DW mobility. The situation is different when the DW is driven by current. The difference is due to the fact that the symmetry changes and the characteristics describing motion for the same parameter sets are significantly different.

Figure 3(b) shows the velocity of a DW in AFC NWs for different values of the applied current, the non-adiabatic parameter β and $M_{s1,2}$. In AFC NW simulations, u corresponds to an effective domain wall mobility defined as $u = (gJ\mu_B P)/(2eM_{s,ave})$ where $M_{s,ave} = (M_{s1} + M_{s2})/2$. In the case of $M_{s1} = M_{s2}$ the Walker breakdown is not encountered for any value of current amplitude for the AFC NW. The torques responsible for triggering the Walker breakdown fully compensate each other.

For both field and current bias, the simulations indicate that the peak velocities and the Walker breakdown threshold are higher for an AFC NW than for single-layer NW. In both cases, the outcome is due to the compensation of different torque terms on account of system symmetry under given bias, which is mediated through the interlayer exchange interaction.

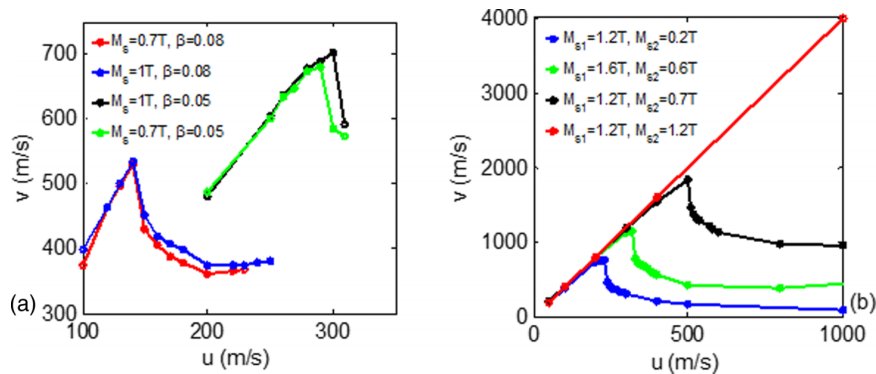


FIG. 3. DW velocity (v) as a function of u obtained via FEM micromagnetic simulations. (a) single-layer NW with different values of the non-adiabatic parameter and saturation magnetization with $\alpha = 0.02$; (b) AFC NW with different values of the saturation magnetization with exchange energy density of 10^{-3} J/m^2 , $\alpha = 0.02$ and $\beta = 0.08$.

To gain a better understanding of this phenomenon, we compared the results to an analytical model.²⁰ The motion of the DW is due to the torques applied on the magnetic moment. By calculating all these torques, it is possible to find the DW velocity and the Walker breakdown limit. This method has been described in detail for a conventional single-layer NW by Mougín.²⁰ It is equally applicable to systems with in-plane and out-of-plane magnetic anisotropies.

In this model, the DWs are considered as two coupled macrospins with the same origin and with saturation magnetizations M_{s1} and M_{s2} , and non-adiabatic STT parameters β_1 and β_2 (Fig. 1(b)). The antiferromagnetic coupling is considered to be infinite (rigid model), such that the two macrospins are oriented perfectly opposite to one another. The cross section of each wire is supposed to be the same. Calculating all the torques applied on the macrospins using spherical coordinates, we can link them to the movement of the DW by using the angular momentum conservation $dL_{\text{total}}/dt = \Gamma_{\text{total}}$. Solving the angular momentum conservation equation for the case of steady DW motion (i.e., motion during which the DW structure does not change) leads to the Walker threshold condition for an AFC NW:

$$\left| H_{\text{W}}^{\text{AFC}} \frac{M_{s1} - M_{s2}}{M_{s1} + M_{s2}} + \frac{\beta_{\text{eff}}}{\gamma \Delta} u_{\text{eff}} \right| = \left| 2\pi\alpha (N_y - N_x) \frac{(M_{s1}^2 + M_{s2}^2)}{(M_{s1} - M_{s2})} \right|, \quad (2)$$

where N_x and N_y are the demagnetizing factors of the volume containing the DW, $\beta_{\text{eff}} = (\beta_1 + \beta_2)/2$ is the effective non-adiabatic parameter, Δ is the length of the DW, $u_{\text{eff}} = (gJ\mu_B P)/(2eM_{s,\text{ave}})$, $M_{s,\text{ave}} = (M_{s1} + M_{s2})/2$, and $H_{\text{W}}^{\text{AFC}}$ is the Walker field for the AFC case. From Eq. (2), it follows that the Walker breakdown is never reached when $M_{s1} = M_{s2}$. On the other hand, Walker breakdown is always present for the single-layer NW case with the Walker threshold condition¹⁹

$$H_{\text{W}}^{\text{single}} + \frac{u}{\gamma \Delta} (\beta - \alpha) = 2\pi\alpha |N_y - N_x| M_{s1}, \quad (3)$$

where $H_{\text{W}}^{\text{single}}$ is the Walker field for the single-layer NW.

The DW velocity in AFC NW for any value of field and current below the Walker breakdown limit is:

$$v = \frac{\gamma \Delta}{\alpha} \left(H \frac{M_{s1} - M_{s2}}{M_{s1} + M_{s2}} + \frac{\beta_{\text{eff}}}{\gamma \Delta} u_{\text{eff}} \right), \quad (4)$$

The DW velocity for the single-layer NW case is given by

$$v = \frac{\Delta \gamma}{\alpha} \left(H + \frac{\beta}{\gamma \Delta} u \right). \quad (5)$$

and it is much lower than that for the AFC NW in Eq. (4).

Equation (2) and Figs. 2(b), 3(b) show that the Walker threshold strongly depends on the respective values of M_{s1} and M_{s2} . As $|M_{s1} - M_{s2}|$ decreases, the Walker breakdown limit is progressively increased, and in principle can be made as large as is allowed by other limitations, such as heat or disorder. The downside is that making the saturation magnetization of both layers very close dramatically reduces the mobility of the DW for the case of field driven DW propagation. However, for the case where only current is applied to the NW, the DW velocity does not depend on the saturation magnetizations and the equation becomes $v = u_{\text{eff}} \beta_{\text{eff}} / \alpha$. Therefore, it is possible to eliminate the Walker breakdown in current operated AFC NWs without impairing the mobility of the DW, thus achieving very high DW velocities.

In conclusion, we have shown that the maximum achievable DW velocity in AFC NWs under field or current bias can far exceed velocities attainable using single-layer NW systems. This result is not a consequence of a reduced average moment of the AFC-NW. We attributed this effect to the particular symmetry of the described system under a given bias, and the consequent compensation of torque terms that are responsible for structural instability. The expressions of these torque terms reflect the fact that interlayer exchange mediates DW dynamics in AFC NWs. It was demonstrated that the Walker breakdown field could be significantly deferred by choosing saturation magnetizations of the two layers to be comparable. The characteristics of DW motion under field and current

bias where demonstrated using micromagnetic simulations, and further justified by an analytical model, which predicts the Walker breakdown field, peak velocity under field and current bias, and wall mobility in AFC systems. It was shown that it is possible to suppress the Walker breakdown limit for current-driven DW motion without affecting its mobility by using similar or identical values of the saturation magnetization in both layers of the AFC NW. This can be done for any value of the damping parameter α or the non-adiabatic spin-transfer torque β .

ACKNOWLEDGMENTS

This work was supported by the NSF grants DMR-1312750 and CCF-1117911, ANR-13-IS04-0008-01 “COMAG” and Partner University Fund ‘Novel Magnetic Materials for Spin Torque Physics’, and European Project (OP2M FP7-IOF-2011-298060) and the Region Lorraine.

- ¹ A. Malozemoff and J. Slonczewski, *Magnetic domain walls in bubble materials* (Academic Press, New-York, 1979).
- ² S. S. P. Parkin, M. Hayashi, and L. Thomas, *Science* **320**, 190 (2008).
- ³ G.S.D. Beach, C. Nistor, C. Knutson, M. Tsoi, and J.L. Erskine, *Nature Mat.* **4**, 741 (2005).
- ⁴ E. Salhi and L. Berger, *J. Appl. Phys.* **73**, 6405 (1993).
- ⁵ J.C. Slonczewski, *J. Magn. Magn. Mat.* **159**, L1 (1996).
- ⁶ L. Berger, *Phys. Rev. B* **54**, 9353 (1996).
- ⁷ D. C. Ralph and M. D. Stiles, *J. Magn. Magn. Mat.* **320**, 1190 (2008).
- ⁸ N. Schryer and J. Walker, *Appl. Phys.* **45**, 5406 (1974).
- ⁹ A. Thiaville, Y. Nakatani, J. Miltat, and Y. Suzuki, *Europhys. Lett.* **69**, 990 (2005).
- ¹⁰ I.M. Miron, T. Moore, H. Szambolics, L.D. Buda-Prejbeanu, S. Auffret, B. Rodmacq, S. Pizzini, J. Vogel, M. Bonfim, A. Schuhl, and G. Gaudin, *Nature Mat.* **10**, 419 (2011).
- ¹¹ A. Thiaville, *Europhys. Lett.* **100**, 57002 (2012).
- ¹² M. Yan, C. Andreas, A. Kákay, F. García-Sánchez, and R. Hertel, *Appl. Phys. Lett.* **99**, 122505 (2011).
- ¹³ H. Saarikoski, H. Kohno, C. H. Marrows, and G. Tatara, *Phys. Rev. Lett.* **104**, 057201 (2010).
- ¹⁴ M. T. Bryan, T. Schrefl, D. Atkinson, and D. A. Allwood, *J. Appl. Phys.* **103**, 073906 (2008).
- ¹⁵ S. Parkin, L. Thomas, and S.-H. Yang, “Domain wall motion in perpendicularly magnetized wires having artificial antiferromagnetically coupled multilayers with engineered interfaces,” US patent 8,687,415 B2, April 1 (2014).
- ¹⁶ R. Chang, S. Li, M. Lubarda, B. Livshitz, and V. Lomakin, *J. Appl. Phys.* **109**, 07D358 (2011).
- ¹⁷ M. Lubarda, *Micromagnetic Modeling and Analysis for Memory and Processing Applications* (2012), 335 pages; 3548304.
- ¹⁸ OOMMF User’s Guide, Version 1.0, M.J. Donahue, and D.G. Porter, Interagency Report NISTIR 6376 (National Institute of Standards and Technology, 1999).
- ¹⁹ A. Thiaville, J. M. Garcia, and J. Miltat, *J. Magn. Magn. Mat.* **242**, 1061 (2002).
- ²⁰ A. Mougín *et al.*, *Europhys. Lett.* **78**, 57007 (2007).